A novel split kinesin assay identifies motor proteins that interact with distinct vesicle populations

Brian Jenkins, Helena Decker, Marvin Bentley, Julie Luisi, and Gary Banker

The Jungers Center for Neurosciences Research, Oregon Health and Science University, Portland, OR 97239

Identifying the kinesin motors that interact with different vesicle populations is a longstanding and challenging problem with implications for many aspects of cell biology. Here we introduce a new live-cell assay to assess kinesin–vesicle interactions and use it to identify kinesins that bind to vesicles undergoing dendrite-selective transport in cultured hippocampal neurons. We prepared a library of "split kinesins," comprising an axon-selective kinesin motor domain and a series of kinesin tail domains that can attach to their native vesicles; when the split kinesins were assembled by chemical dimerization, bound vesicles were misdirected into the axon. This method provided highly specific results, showing that three Kinesin-3 family members—KIF1A, KIF13A, and KIF13B—interacted with dendritic vesicle populations. This experimental paradigm allows a systematic approach to evaluate motor–vesicle interactions in living cells.

Introduction

Long-range intracellular vesicle transport toward the plus end of microtubules is principally performed by kinesin family motor proteins. All kinesin family members are structured similarly, with a globular "motor domain" that uses ATP hydrolysis to translocate along microtubules and a "tail domain" that interacts with cargoes, which can include organelles and membrane vesicles, RNA and protein complexes, and other microtubules (Hirokawa et al., 2010). Although the mechanics of motor domain translocation are now relatively well understood, much less is known about how kinesins interact with their cargoes and how kinesin–cargo interactions direct transport to the correct intracellular destinations.

Nerve cells offer a notable example of the importance of these questions. In neurons, directed kinesin-mediated transport is thought to be crucial for the maintenance of neuronal polarity, ensuring that axons and dendrites acquire their correct complement of membrane proteins. Live-cell imaging of cultured neurons shows that microtubule-based transport is selective: vesicles containing dendritic membrane proteins are transported efficiently into the dendrites but do not enter the axon (Burack et al., 2000; Silverman et al., 2001); vesicles containing axonal membrane proteins are not excluded from dendrites, but their transport is biased toward the axon (Burack et al., 2000; Nakata and Hirokawa, 2003). Before the basis of this selectivity can be understood, we need to know the full complement of kinesins that are responsible and how their movements are regulated. Present understanding of these questions is fragmentary, at best.

Solving the "cargo problem" (Terada and Hirokawa, 2000)—that is, determining which kinesins move which cargoes—is challenging because cells express so many different kinesins and contain so many different vesicle populations, to say nothing of other cargoes. To date, two broad approaches have been used to address the cargo problem (Hirokawa and Noda, 2008; Hirokawa et al., 2010). Yeast two-hybrid and immunoprecipitation strategies have identified biochemical interactions between kinesins and many putative cargo proteins or adaptor molecules. Although this approach has yielded many kinesin binding partners, it is not able to provide information about these interactions in vivo, where kinesin–vesicle interactions may be transient and highly regulated. An alternative strategy involves disrupting the function of specific kinesin motors using dominant-negative or RNAi approaches, then examining changes in the expression or localization of presumptive cargo proteins. These approaches require long expression times of the interfering constructs, which can lead to nonspecific secondary effects. In the likely case that a vesicle can be carried by multiple kinesins, false-negative results can only be avoided by coexpressing a large set of constructs. Even when all of these strategies are applied in combination, it is difficult to obtain a complete and

B. Jenkins, H. Decker, and M. Bentley contributed equally to this paper.

Correspondence to Gary Banker: bankerg@ohsu.edu

Abbreviations used in this paper: FRB, FKBP12–rapamycin binding; LDLR, low-density lipoprotein receptor; TfR, transferrin receptor.

The Rockefeller University Press $30.00
J. Cell Biol. Vol. 198 No. 4 749–761
www.jcb.org/cgi/doi/10.1083/jcb.201205070

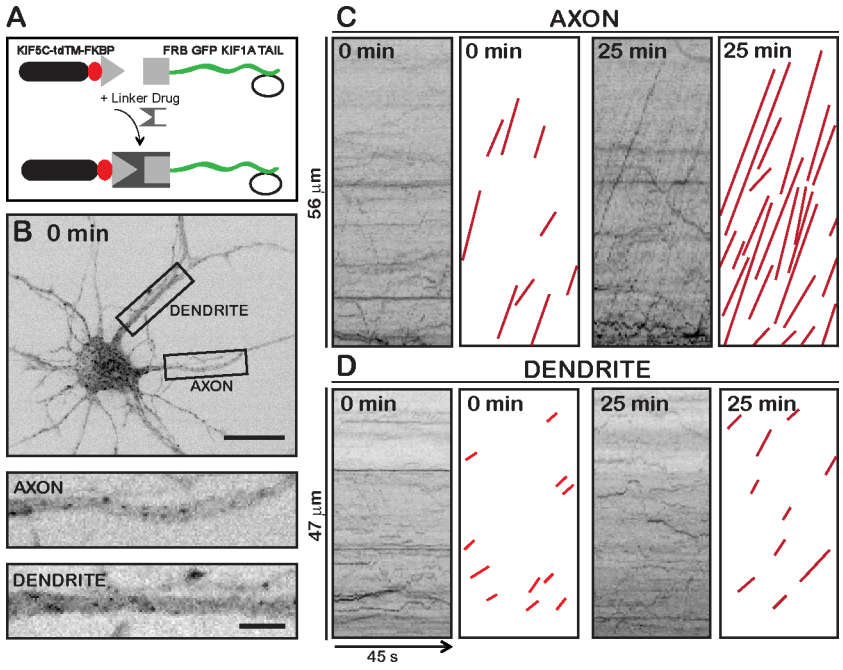

Figure 1. **Linking a kinesin tail–vesicle complex to an active axon-selective motor domain causes a distinctive increase in axonal vesicle transport.** (A) Hippocampal neurons were transfected with a split kinesin consisting of an FRB-GFP-KIF1A tail, which interacts with endogenous vesicles, and the KIFC^{559}-tdTM-FKBP motor domain. The constructs were expressed for 18 h before live imaging to evaluate the transport of KIF1A-labeled vesicles. (B) Before addition of linker drug, the FRB-GFP-KIF1A–labeled vesicles were present in both the axon and the dendrites. In this and all subsequent figures, the contrast was inverted so that brightly labeled vesicles appear dark. Bars: (top panels) 20 µm; (high magnification panels) 5 µm. (C and D) Kymographs illustrate the transport of KIF1A-labeled vesicles before (0 min) and 25 min after addition of 1 µM AP 21967. Before addition of the linker, labeled vesicles were transported bi-directionally in the axon and the dendrites. After addition of the linker drug, there was a pronounced increase in long-range anterograde events in the axon. Graphs with red lines illustrate all anterograde events visible on the corresponding kymographs. In the kymographs, time is shown on the x axis and position along the neurite on the y axis. Diagonal lines with positive slope represent movements away from the cell body. Time and distance calibration are the same for all kymographs. See also Video 1.

comprehensive picture of the kinesins that transport a given cargo, and conflicting results are not unusual.

Here we introduce a novel strategy—the split kinesin method—that potentially can identify all of the kinesins that interact with a given fluorescently labeled vesicle population. This method entails the expression of separate constructs encoding a kinesin tail and a kinesin motor domain that can be assembled into a complete kinesin using a linker drug. The kinesin tail binds vesicles, but is incapable of influencing their movement because it lacks a motor domain; the motor domain walks constitutively along microtubules, but cannot move vesicles because it lacks a cargo-binding domain. When the two components are linked together, their assembly leads to a rapid and profound change in the trafficking pattern of only those vesicles that bind the expressed kinesin tail domain.

To demonstrate the application of this method, we use it to determine the kinesins responsible for selective dendritic transport in neurons. We identify three members of the Kinesin-3 family—KIF1A, KIF13A, and KIF13B—that are implicated in the transport of the dendritically polarized cargoes transferrin receptor (TfR) and low-density lipoprotein receptor (LDLR). For both cargoes tested, we identified two different kinesins that interact with the same vesicle population. Prior results implicate KIF1A in the transport of AMPA receptors (Shin et al., 2003), but the role of KIF13A and KIF13B in dendritic transport has not been previously suspected. Intriguingly, two of the three dendritic kinesins also mediate the axonal transport of other vesicle populations, confirming the hypothesis that kinesins can be steered to the axon or the dendrites depending on whether they interact with an axonal or a dendritic cargo (Setou et al., 2002).

Results

To address the cargo problem, we sought an unbiased, systematic approach capable of identifying the kinesins that contribute to the transport of a given population of vesicles, even if multiple kinesins participate. The idea we chose to explore involved creating an expression library of all of the kinesin tails that might bind a given vesicle population, then developing an assay that resulted in a change in vesicle trafficking only when an expressed tail binds to the vesicle in question. This led to the split kinesin strategy, which allows the expressed kinesin tails to bind an endogenous vesicle population that has been labeled with a fluorescent marker, then links the tails to a constitutively active kinesin motor domain, resulting in a distinctive increase in vesicle movement. The method uses the motor domain of the Kinesin-1 family member KIF5C, whose properties have been well characterized (Hirokawa et al., 2010). When expressed in neurons, the KIF5C motor domain translocates into the axon with high efficiency (Jacobson et al., 2006; Verhey et al., 2011). A series of kinesin tails are fused to the FKBP12–rapamycin-binding (FRB) domain, which can be linked to the constitutively active KIF5C fused to the FKBP domain by addition of the linker drug AP21968, a rapamycin analogue (Belshaw et al., 1996). Kapitein et al. (2010) showed that linking a motor protein to a peroxisomal membrane protein using the FKBP-FRB strategy induced a pronounced increase in peroxisome movement. Using an inducible linker rather than constructing a series of chimeric kinesins provides the advantage that the same cell can be examined before and shortly after creating the active motor protein.

Although the split kinesin strategy is conceptually straightforward, we were uncertain if enough copies of the expressed motor domain will be present in the cell body to link to the expressed tail or if enough copies of the tail will bind the vesicles to alter their movements. As a proof of principle, we attempted to alter the behavior of the vesicles that bind the tail domain of KIF1A. Shin et al. (2003) have shown that GFP-KIF1A labels a specific population of neuronal vesicles that are transported in axons and dendrites. We expressed a GFP-KIF1A tail that had been fused to the FRB domain together with the

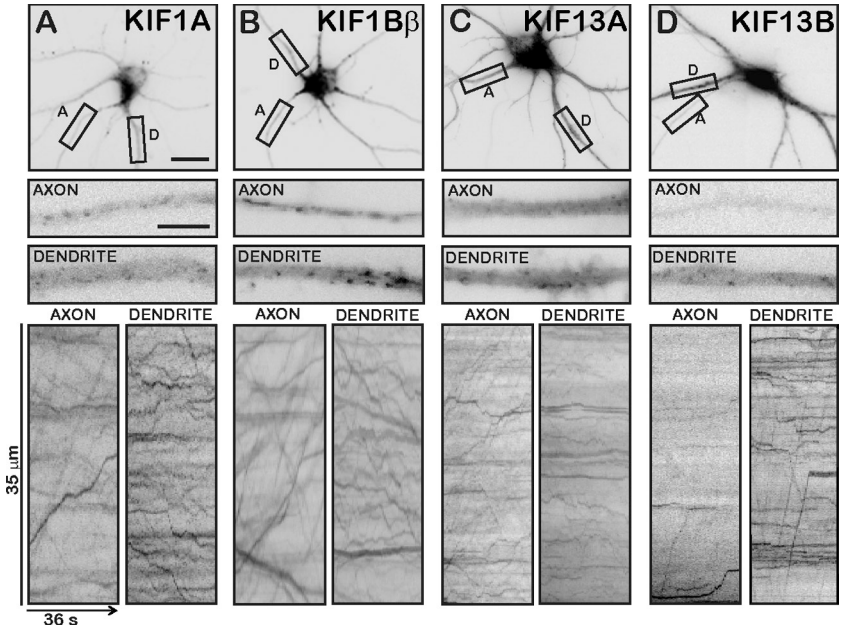

Figure 2. **Transport characteristics of vesicles labeled by expressing full-length GFP-tagged Kinesin-3 motors.** Fluorescently labeled full-length kinesins were expressed in cultured hippocampal neurons to label vesicles. (A–D) Representative images of axons and dendrites of hippocampal neurons expressing GFP-tagged KIF1A, KIF1Bβ, KIF13A, and KIF13B, respectively. Boxed regions showing high magnification views of a portion of the axon and a dendrite are shown below. Kymographs illustrating vesicle movements in the boxed regions show that vesicles labeled with KIF1A, KIF1Bβ, and KIF13A were transported bi-directionally in both axons and dendrites. In contrast, vesicles labeled with KIF13B were largely polarized to the dendrites. Bars: (top panels) 20 µm; (high magnification panels) 5 µm. Time and distance calibration are the same for all kymographs.

KIF5C motor domain fused to FKBP (Fig. 1 A). The motor domain used in all experiments is KIF5C^{559}-tdTM-FKBP. Expression of the GFP-KIF1A construct resulted in the labeling of vesicles in the axon and in dendrites (Fig. 1 B; in this and all subsequent figures, the contrast has been reversed so that fluorescent objects appear dark on a light background). Kymographs before addition of the linker drug showed vesicles moving bi-directionally in both the axon and the dendrite (Fig. 1, C and D). In kymographs, moving vesicles give rise to diagonal lines; lines with a positive slope represent movements away from the cell body. Before the addition of linker drug, vesicles moved in both the axon and dendrites. The movements were relatively short, especially in the dendrites where vesicles seldom traveled more than 10–15 µm. The amount of transport was similar to that in cells expressing full-length GFP-KIF1A (see Fig. 2 A), which indicates that expression of this kinesin tail does not act as a dominant negative. After adding the linker drug, the axonal transport of KIF1A-labeled vesicles increased markedly (Fig. 1 C). A continuous stream of vesicles entered the axon and moved for long distances without pauses or reversals (Video 1). The increase in transport began ∼15 min after treatment and peaked between 20 and 30 min. In the dendrites there was no apparent increase in transport, consistent with the observation that KIF5C^{559} translocates preferentially to axon tips (Huang and Banker, 2011). This result shows that it is possible to change the trafficking behavior of cargo vesicles by allowing the appropriate kinesin tail domain to interact with a specific vesicle population and chemically linking this tail to a constitutively active motor domain. It is noteworthy that a change in transport can be induced after as little as 15 min of exposure to the linker drug.

Vesicle populations labeled by GFP-tagged Kinesin-3 family members

Neurons express some 15 different kinesins thought to mediate vesicle or organelle transport (Silverman et al., 2010). In a screen to identify candidate kinesins that mediate axon- or dendrite-selective transport, Huang and Banker (2011) expressed constitutively active motor domains of all these kinesins in cultured neurons. This work demonstrated that most kinesin motor domains accumulate only in axonal tips (Nakata and Hirokawa, 2003; Jacobson et al., 2006; Nakata et al., 2011). However, the Kinesin-3 family members KIF1A, KIF1Bβ, and KIF13B accumulate in both axon and dendrite tips, as does the Kinesin-4 family member KIF21B (Huang and Banker, 2011). These results indicate that members of the Kinesin-3 and Kinesin-4 families merit investigation as potential motors for dendritically polarized vesicles.

To further explore this possibility, we expressed full-length, N-terminally GFP-tagged versions of these kinesins in cultured hippocampal neurons in order to observe the localization and movements of vesicles they labeled. Although most kinesins do not label vesicles, some members of the Kinesin-3 family label vesicles well enough for live-cell imaging (Lee et al., 2003). Fig. 2 shows representative examples of cells expressing GFP-tagged members of the Kinesin-3 family. The corresponding kymographs show the movement of the labeled vesicles in these cells and compare their patterns of transport. The most consistent vesicle labeling was seen after expression of KIF1A and KIF1Bβ, but in favorable cases it was possible to image vesicles labeled by KIF13A and KIF13B. KIF1A, KIF1Bβ, and KIF13A all labeled vesicles that were transported bi-directionally in axons and dendrites (Fig. 2, A–C). In contrast, vesicles labeled with KIF13B were largely polarized to the dendrites (Fig. 2 D). During live recordings, KIF13B-labeled vesicles rarely entered the axon, but were transported efficiently in the somatodendritic domain of the cell. GFP-tagged Kinesin-4 family members showed a diffuse distribution when expressed in cultured neurons, making it impossible to observe vesicle behavior (not depicted).

These results indicate that KIF13B could be a purely dendritic vesicle motor. The remaining Kinesin-3 motors likely mediate transport of both dendritic and axonal cargo, but are not inherently targeted to a particular domain of the cell.

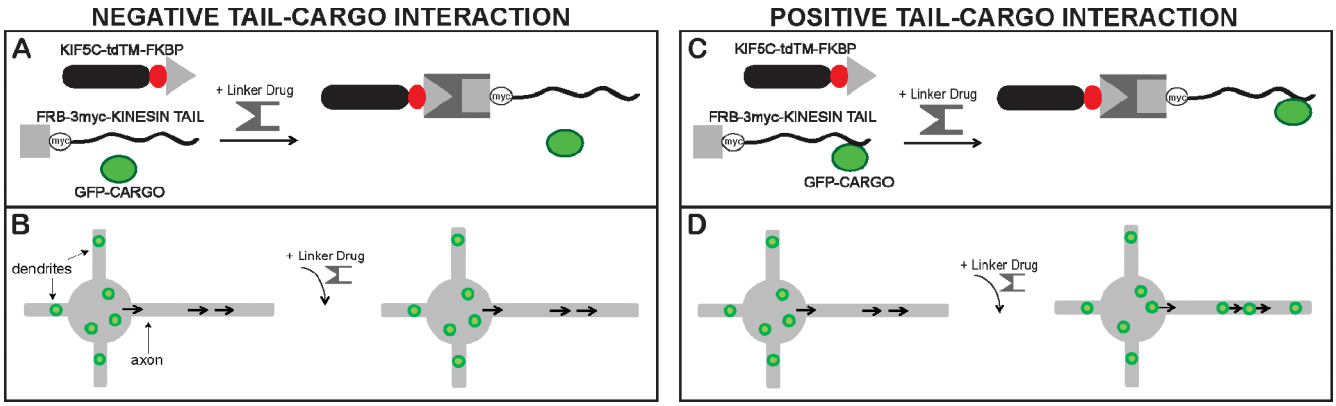

Figure 3. **Schematic diagram illustrating the split kinesin assay.** (A) Three constructs are expressed together: a vesicle marker labeled with GFP, a constitutively active axon-selective kinesin motor domain tagged with tdTomato and fused to FKBP (KIF5C^{559}-tdTM-FKBP), and a myc-tagged kinesin tail domain fused to FRB. The kinesin tail domain binds its endogenous cargo vesicle, but co-assembles with the kinesin motor domain only after addition of the linker drug. (B) In the absence of linker drug, endogenous motor proteins transport GFP-labeled vesicles in dendrites, but they do not enter the axon. The constitutively active motor domain (black arrows) translocates toward the axonal tip, but does not bind cargo. After the linker drug is added, the split kinesin is assembled, but without interaction between the kinesin tail and the labeled vesicle population, this does not result in any changes in the transport behavior of the vesicles. (C) In case of a positive interaction between the tail and the vesicle, the tail is able to bind the vesicle population immediately after expression. After the addition of linker drug the split kinesin is assembled on the labeled vesicle. (D) Upon the addition of the linker drug, GFP-labeled vesicles that bind the expressed kinesin tail become attached to the constitutively active axonal KIF5C^{559}-FKBP motor domain, which transports them into the axon.

Split kinesin tail constructs express at comparable levels and exist primarily in a soluble pool

Fig. 3 shows how the split kinesin strategy is applied to identify kinesin–cargo interactions in neurons. In the absence of the linker drug, KIF5C^{559}-FKBP translocates into the axon, but this does not affect vesicle transport because this construct is unable to bind the labeled cargo vesicle (Fig. 3 A). The kinesin tail attaches to its natural vesicle population, but this does not lead to vesicle transport because it lacks a motor domain. After the linker drug is added, the transport pattern of vesicles that do not bind the expressed kinesin tail is not altered (Fig. 3 B). In contrast, vesicles that carry the kinesin tail become linked to the constitutively active motor domain (Fig. 3 C), which results in an increase in their transport into the axon (Fig. 3 D).

To change the transport behavior of a given vesicle population using the split kinesin paradigm, it is necessary that the cargo-binding tails are all expressed at sufficient levels. Each split kinesin tail construct consisted of the N-terminal FRB domain, a linker consisting of three myc tags, and the kinesin tail. To confirm expression levels, tails were expressed in cultured hippocampal neurons, which were stained for myc after fixation. Immunostaining for the expressed tails was present throughout the cell body and dendrites and extended far into the axon, much like soluble GFP. The tails of KIF1A, KIF13B, and KIF1Bα also labeled vesicles, but even for those tails the staining showed a primarily soluble distribution (not depicted). The KIF13B tail was enriched in dendrites (Fig. 4 A), similar to the full-length construct (Fig. 2 D). Although the split kinesin tails were present throughout the cell, the KIF5C^{559}-FKBP motor domain was highly concentrated at the tip of the axon and axonal branches (Fig. 4 B), as is KIF5C^{559} lacking the FKBP domain (Jacobson et al., 2006). Adding the linker drug did not cause an appreciable change in the distribution of either the expressed tail or the kinesin motor domain.

The expression levels of the different tails were quantified by measuring the average intensity of anti-myc staining in the nerve cell body. Fig. 4 C shows the expression levels for all of the split kinesin tails that were used in our screen. The screen included all five members of the Kinesin-3 family that are expressed at high levels in neurons, including both of the prominent splice variants of KIF1B (Materials and methods; Table 1). We also included three other kinesins that have been implicated in dendritic transport: the conventional Kinesin-1 family member KIF5C, which is thought to interact with AMPA receptors (Setou et al., 2002); the Kinesin-2 family member KIF17, which has been implicated in the dendritic transport of NMDA receptor subunits and the $Kv_{4.2}$ potassium channel (Setou et al., 2000; Chu et al., 2006); and KIF21B, the Kinesin-4 family member that accumulates at both dendritic and axonal tips in the truncated kinesin expression assay (Huang and Banker, 2011). All of the split kinesin tails were present at readily detectable levels. For any given FRB-tail, there was a considerable range in expression level from cell to cell, but the average expression levels of the different tails varied by less than threefold. Thus, it is safe to assume that the FRB-kinesin tails are expressed at high enough levels to interact with their endogenous binding partners.

KIF13A and KIF13B bind transferrin receptor vesicles

Having established the feasibility of this approach, we attempted to use this strategy to identify the kinesin tails that interact with vesicles that undergo dendrite-selective transport. Compared with most axonal vesicles, dendrite-selective vesicles are small and dim and the presence of labeled proteins undergoing synthesis in the dendritic rough endoplasmic reticulum increases background labeling. We chose to label dendritic vesicles by expressing GFP-tagged transferrin receptor (TfR), which provides a comparatively high signal-to-noise ratio, making it possible to image extensive transport in dendrites (Burack et al., 2000; Silverman et al., 2001). TfR is highly polarized to

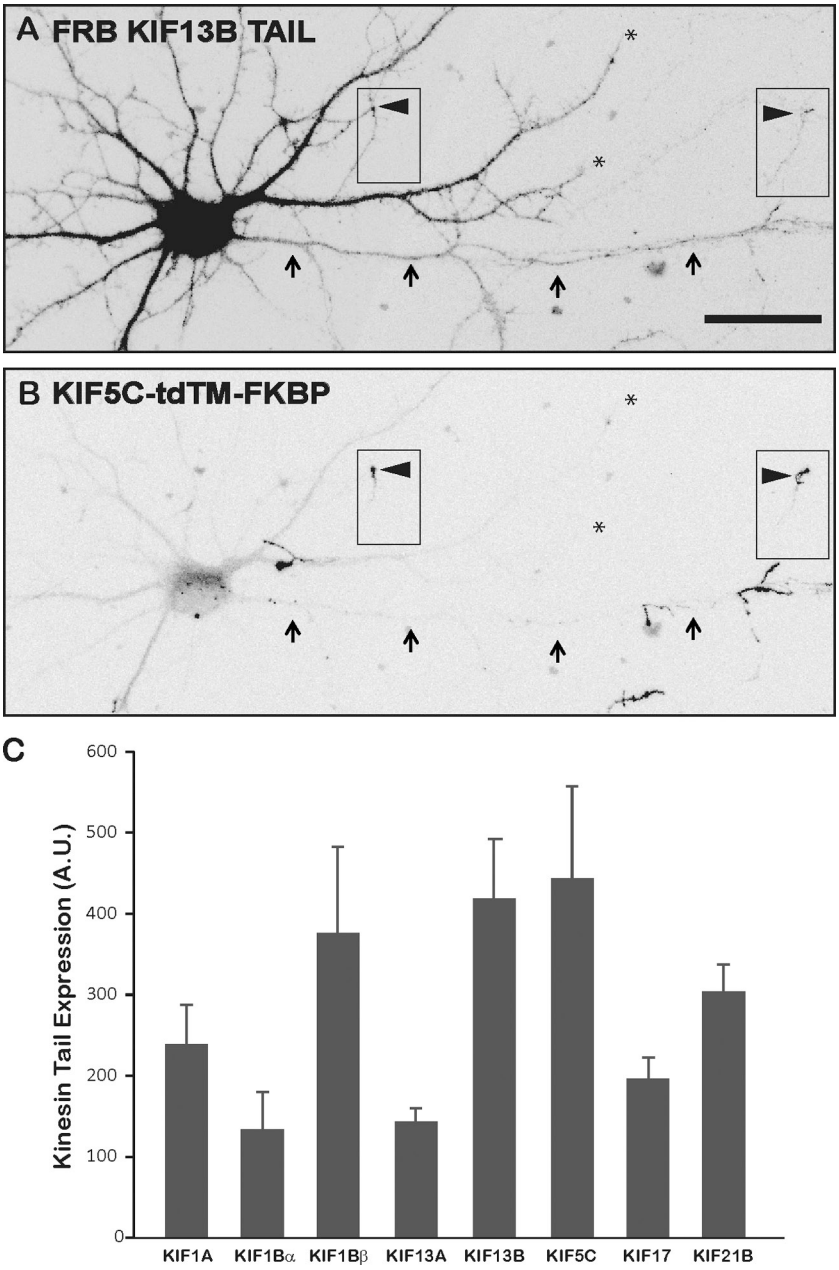

Figure 4. **Localization and level of expression of the split kinesin components.** (A and B) A cell co-expressing a split kinesin tail (FRB-myc-KIF13B tail) and the KIF5C^{559}-tdTM-FKBP motor domain. Immunostaining for the kinesin tail was present throughout the cell body and dendrites and extended far into the axon (arrows). The motor domain was concentrated at the tips of axonal branches (arrowheads) but not at dendritic tips (asterisks). (C) Comparison of the expression levels of the different split kinesin tails (based on anti-myc immunostaining). Average intensity of staining in the cell body was measured for at least 15 cells from two separate experiments in each condition. Bar, 20 µm.

dendrites in both vertebrate and invertebrate neurons, which is reflected in the movement of TfR-containing vesicles; more than ten times as many vesicle movements are observed in a typical dendrite compared with the axon (Jareb and Banker, 1998; Burack et al., 2000; Silverman et al., 2001; Henthorn et al., 2011). Vesicles labeled with TfR-GFP are thought to contain other dendritically polarized proteins as well, including AMPA receptors (Kennedy et al., 2010).

To identify kinesins that bind TfR vesicles, we coexpressed KIF5C^{559}-FKBP and a series of kinesin tails that had an N-terminal FRB domain and a myc tag (Fig. 5 A). Staining for myc confirmed that more than 90% of cells that were labeled with TfR-GFP coexpressed all three constructs (not depicted). Cells were then recorded before and after the addition of linker drug.

Fig. 5 D shows a cell expressing TfR-GFP, KIF5C^{559}-FKBP, and the FRB-tagged tail of KIF13B, a member of the Kinesin-3 family. Before adding the drug there was robust dendritic transport of TfR, but little transport in the axon (Fig. 5, B and C). There is a small population of dim vesicles that exist in the axon, but almost all of the brightly labeled carriers were restricted to the somatodendritic region of the cell. By 9 min after drug addition, the transport pattern showed a pronounced increase in vesicles undergoing high velocity, long-range anterograde movement in the axon. The trafficking increase reached its maximum between 16 and 23 min (Fig. 5 C; Video 2). Interestingly, the overall intensity of the proximal axon also increased during this period, as can be seen in the kymographs and the still image (Fig. 5 D).

Fig. 5 (E–L) shows kymographs representing axonal transport of TfR-GFP in cells expressing a series of different split kinesins. Before adding the linker drug there was dendritic TfR transport in all cells, which demonstrates that expression of

Table 1. **Kinesin tail constructs**

Family	Subfamily	Tail construct (aa)	Genbank/EMBL/DDBJ accession no.
Kinesin-1	KIF5C	378–955	NM_001107730
Kinesin-2	KIF17	400–1040	NM_010623
Kinesin-3	KIF1A	395–1695	NM_008440
Kinesin-3	GFP-KIF1A	680–1695	NM_008440
Kinesin-3	KIF1Bα	386–1167	NM_008441
Kinesin-3	KIF1Bβ	386–1770	NM_207682
Kinesin-3	KIF13A	361–1750	NM_010617
Kinesin-3	KIF13B	362–1827	NM_001081177
Kinesin-4	KIF21B	410–1668	NM_001039472

these kinesin tails did not result in dominant-negative effects. After adding the linker, both KIF13A and KIF13B tails gave a strong positive interaction with TfR vesicles, as indicated by the marked enhancement in anterograde axonal transport (Fig. 5, H and I). Based simply on inspection of the recordings, a clear increase in transport was observed in 55% of cells expressing KIF13A and 65% of cells expressing KIF13B. Given the complexity of the assay, which requires expression of multiple constructs and chemical cross-linking between constructs, it is not surprising that some cells expressing KIF13A or KIF13B tails yielded negative results. Expression of KIF1A, KIF1Bα, KIF1Bβ, KIF5C, KIF17, and KIF21B tails all failed to produce any detectable increase in the movement of TfR vesicles in any cells (Fig. 5, E–G and J–L). This result demonstrates the high specificity of this experimental paradigm.

To quantify changes in transport of TfR vesicles in cells expressing different tails, we prepared kymographs of vesicle transport before and 20–30 min after adding the linker drug. To reduce the possibility of false-negative results, cells were included in this analysis only if TfR was well polarized (to ensure that an increase in axonal traffic would be obvious) and if the cell displayed robust dendritic transport both before and after addition of the linker drug (to ensure that the transport machinery was fully functional). The results are shown in Fig. 6, which indicates the difference in the number of anterograde events observed in the axon after adding the linker drug for each of the expressed tails. There was a prominent, statistically significant increase in axonal transport in cells expressing KIF13A and KIF13B. In cells expressing the other kinesin tails there was a small decrease in transport 20–30 min after adding the linker drug. This likely reflects a slight inhibition of transport due to phototoxicity as a result of the extensive imaging required to quantify transport (typically 180–240 exposures over 30 min).

Low-density lipoprotein receptor vesicles interact with KIF1A and KIF13B

To further explore the utility of the split kinesin assay we used this strategy to identify the kinesins that interact with vesicles carrying a different dendritic cargo protein, low-density lipoprotein receptor (LDLR). LDLR is not endogenously expressed by hippocampal neurons, but when expressed it is highly polarized to the dendritic surface and vesicles labeled by GFP-tagged LDLR undergo dendrite-selective transport (Jareb and Banker, 1998; Silverman et al., 2001). TfR and LDLR are thought to leave the Golgi in the same vesicles, based on analysis of their sorting signals, but their endocytic recycling pathways diverge (Jareb and Banker, 1998; Gan et al., 2002; May et al., 2007).

We expressed GFP-LDLR and KIF5C^{559}-FKBP with the same series of FRB-kinesin tails, and then looked for a change in trafficking after addition of linker drug (Fig. 7). Representative kymographs from this series of experiments confirm the extremely high specificity of this experimental approach (Fig. 7, B–I). Only cells expressing KIF1A and KIF13B tails showed the characteristic increase of axonal transport that signifies a tail–vesicle interaction (Fig. 7, B and F). The remaining kinesins that were tested, KIF1Bα, KIF1Bβ, KIF13A, KIF21B, KIF17, and KIF5C failed to cause a change in transport (Fig. 7, C–E and G–I). Based on inspection of the recordings, all cells expressing KIF1A (8 of 8) and 72% of cells expressing KIF13B showed a clear increase in LDLR vesicles entering the axon when the linker drug was added. One of ten cells expressing the KIF13A tail was positive. All of the remaining tails yielded exclusively negative results.

Quantification of these results based on kymograph analyses are shown in Fig. 7 J. A statistically significant increase in the number of anterograde movements of LDLR vesicles was observed in cells expressing KIF1A and KIF13B tails. No significant changes in transport were observed in cells expressing other tails. These results again document the selectivity of this assay.

Because vesicles labeled by GFP-LDLR, but not TfR-GFP interact with KIF1A and the reverse is true for KIF13A, these two pools of vesicles cannot be identical. Because TfR and LDLR differ in some aspects of their endosomal recycling it is possible that this is reflected in the differential binding observed with KIF1A and KIF13A. However, a subpopulation of endosomes contains both TfR and LDLR and this population may be moved by KIF13B (Maxfield and McGraw, 2004).

Altered kinesin-driven transport of TfR vesicles causes TfR to recycle through the axonal plasma membrane

Having identified kinesin tails that interact with dendritic vesicles, we wanted to determine if prolonged activation of a split kinesin can lead to a detectable increase in dendritic proteins in the axon and whether the mistargeted vesicles are capable of fusing with the membrane and delivering dendritic proteins to the axonal surface. To address these questions, cells expressing TfR-GFP,

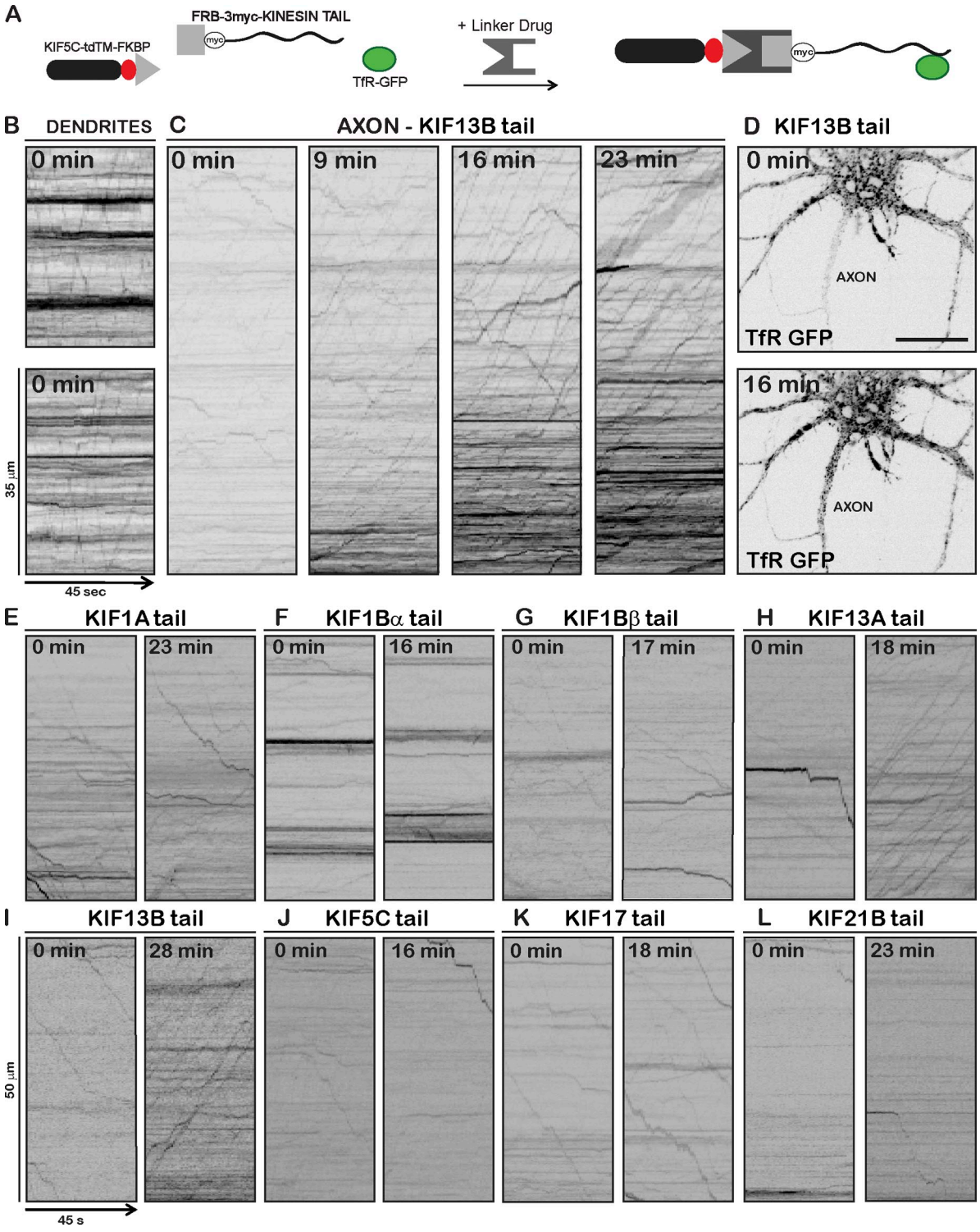

Figure 5. **KIF13A and KIF13B tails bind transferrin receptor vesicles.** (A) A schematic showing the three constructs expressed in this assay before and after assembly of the split kinesin. (B) Kymographs showing the transport of TfR vesicles in dendrites before assembly of the split kinesin in two different dendrites. (C) Kymographs showing the transport of TfR vesicles in the axon before and at varying times after adding the linker drug (AP 21967, 1 µM) in a cell expressing the FRB-KIF13B tail. Before adding the linker drug there was far less vesicle transport in the axon than the dendrites (compare with B). After drug-induced assembly of the split kinesin there was a pronounced increase in long-range anterograde vesicle transport in the axon. Time and distance calibration are the same for kymographs in B and C. (D) Images showing the cell body and proximal axon of the neuron imaged immediately before (0 min) and after 16 min of treatment with linker drug. Note the increase in intensity of TfR-GFP in the axon after 16 min. Bar, 20 µm. (E–L) Kymographs illustrating axonal transport of TfR-GFP vesicles in hippocampal neurons expressing different split kinesin tail constructs. The kymographs show the transport of TfR vesicles in the axon before (0 min) and 14–28 min after addition of the linker drug. There was no change in the overall transport of TfR vesicles when KIF1A, KIF1Bα, KIF1Bβ, KIF5C, KIF17, or KIF21B tails were expressed. In contrast, there was a large increase in the long-range anterograde transport events of TfR vesicles when KIF13A (H) or KIF13B (I) tails were used. See also Video 2. Time and distance calibrations are the same for kymographs in E–L.

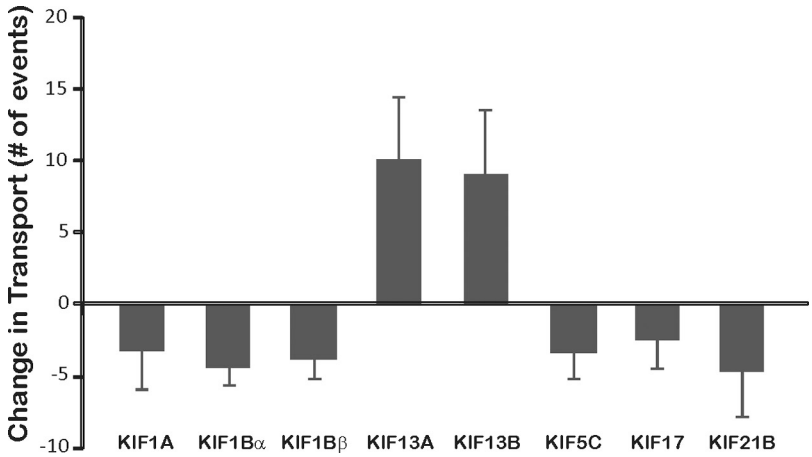

Figure 6. **Quantification of changes in TfR vesicle traffic in neurons expressing different split kinesin tails.** The figure plots the difference in the amount of anterograde transport before and 15–30 min after adding linker drug (number of anterograde events after drug minus number of anterograde events before drug; mean ± SEM). A statistically significant increase in axonal transport of TfR vesicles was observed in cells expressing FRB-KIF13A and FBR-KIF13B tails (Wilcoxon signed rank test; $P < 0.01$). $n = 7$–16 cells per condition.

KIF5C^{559}-FKBP, and FRB-KIF13B tail were treated with linker drug for 4 h. The total amount of TfR-GFP in the axon was assessed by measuring GFP fluorescence and the TfR-GFP that was capable of cycling between the cell surface and axonal endosomes detected by staining living cells with antibodies against GFP (which was present in the ectodomain of TfR). Fig. 8 A shows a control cell (not exposed to the linker drug) and a treated cell. The control cell displayed strong GFP fluorescence in the dendrites but not the axon. Exposing the intact cell to antibody also revealed extensive dendritic staining, indicating that the expressed TfR-GFP was capable of cycling between endosomes and the dendritic surface. A higher magnification view of the boxed region shows how little TfR was present in the axon. In the cell treated with linker drug for 4 h, a strong punctate TfR signal was present in the axon as well as in the dendrites. The high magnification inset shows that there was an increase in the diffusely distributed signal, which likely represents TfR present on the axonal surface, as well as an accumulation of TfR in punctuate structures in the axon. Many of these latter objects probably represent endosomes that formed while the cells were exposed to anti-GFP antibody.

Fig. 8 B shows line-scan quantifications of the boxed region of the axon for the control and treated cells. Although there is little variation in intensity along the axon of control cells, the 4 h-treated cells show a strong increase in punctuate fluorescence of TfR-GFP. Most peaks in the control cell are lower than the minimum brightness of the treated cell and the maxima in the treated axon are up to sixfold higher than those of the untreated control. Staining living cells with an antibody to detect TfR that cycled through the cell surface showed a comparable increase, demonstrating that TfR vesicles fuse with the plasma membrane when they are misdirected to the axon.

Quantitative analysis of 28 cells shows that linking KIF13B tail to KIF5C motor domain significantly increased both total axonal TfR and TfR exposed on the axonal surface (Fig. 8 C). Although there were treated cells with TfR levels that fell within the control range, in most cases there was a marked increase in axonal TfR. This result is consistent with the live-cell assays, in which axonal transport increases were seen in only ∼65% of cells.

These results confirm that the KIF13B split kinesin can misdirect TfR, causing it to accumulate in the axon over time. But more importantly, they show that vesicles containing dendritic proteins are capable of fusing with the plasma membrane if they enter the axon. There is no fail-safe mechanism to prevent mistargeted vesicles from delivering dendritic proteins to the axonal surface. Thus, selective dendritic transport plays a crucial role in preventing dendritically polarized proteins from reaching the incorrect cellular domain.

Discussion

A new method for elucidating kinesin–vesicle interactions

In the experiments presented here we introduce a new method to identify kinesin–vesicle interactions in living cells and use it to identify three Kinesin-3 family members that bind to vesicles containing dendritically polarized proteins. The split kinesin assay reveals the high degree of selectivity that governs kinesin–vesicle interactions. For example, KIF1A binds vesicles labeled by LDLR-GFP and pulls them into the axon after split kinesin assembly, but the closely related family members KIF1Bα and KIF1Bβ yielded entirely negative results in this assay. Likewise, the highly homologous kinesins KIF13A and KIF13B exhibit distinct vesicle-binding specificities. The split kinesin assay provides a unique perspective on kinesin–cargo selectivity because it can be used to probe interactions between a defined vesicle population and a broad range of kinesins. Defining how specific motors are selectively linked to their vesicular cargoes remains a challenging problem (Akhmanova and Hammer, 2010), and current methods do not allow an unbiased evaluation of interactions between a given vesicle population and all relevant kinesin family members.

In principle, the split kinesin assay is capable of identifying the kinesins that interact with any fluorescently labeled vesicle population in any cell type, so long as linking the vesicles to a constitutively active motor domain will result in a distinctive pattern of transport. One advantage of this method is the high specificity with which it detects kinesin–vesicle interactions. Of the sixteen possible tail–vesicle combinations tested in our screen, only four combinations yielded a positive readout. Interactions that were scored as positive caused a pronounced increase in transport in 55–90% of recorded cells. This is a striking result because there was essentially no axonal transport of these vesicles in the same cells before assembling the split kinesins.

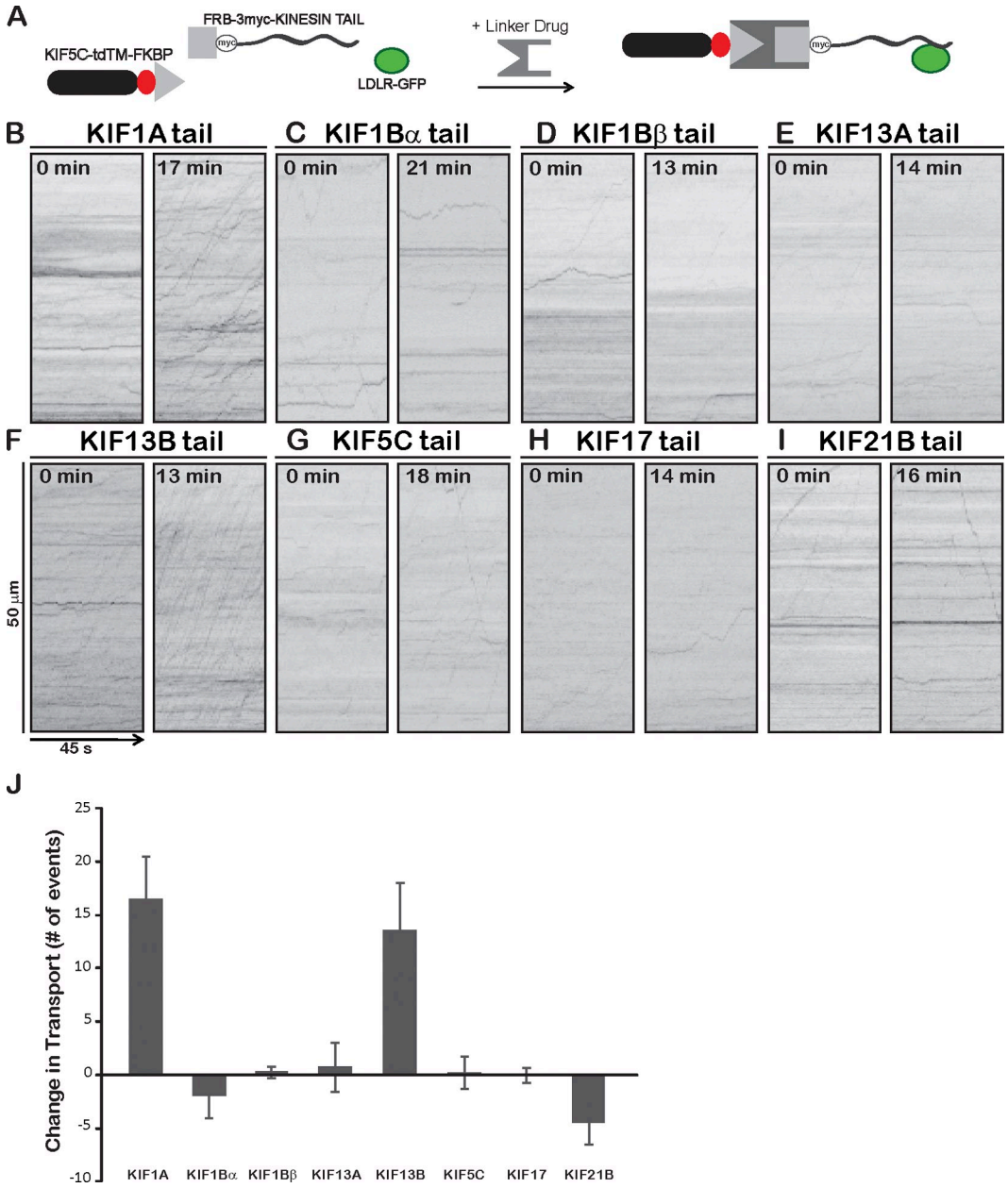

Figure 7. **KIF1A and KIF13B tails bind low-density lipoprotein receptor vesicles.** (A) The three constructs expressed in this assay before and after assembly of the split kinesin. (B–I) Kymographs illustrating axonal transport of LDLR-GFP vesicles in hippocampal neurons expressing different split kinesin tail constructs. The kymographs show the transport of LDLR vesicles in the axon before (0 min) and 13–21 min after addition of the linker drug. There was no change in the overall transport of TfR vesicles when KIF1Bα, KIF1Bβ, KIF13A, KIF5C, KIF17, or KIF21B tails were expressed. In contrast, there was a large increase in the long-range anterograde transport events of LDLR vesicles when KIF1A (B) or KIF13B (F) tails were used. (J) The difference in the amount of anterograde transport before and 15–30 min after adding linker drug (number of anterograde events after drug minus number of anterograde events before drug; mean ± SEM). A statistically significant increase in axonal transport of LDLR vesicles was observed in cells expressing FRB-KIF1A and FRB-KIF13B tails (Wilcoxon signed rank test; $P < 0.01$). $n = 7$–11 cells per condition. Time and distance calibration are the same for all kymographs.

Conceivably, overexpression of a kinesin tail could enable it to bind vesicles nonspecifically, but the selectivity of the kinesin binding observed in these experiments suggests that this is unlikely.

The likelihood of false negatives in this assay is more difficult to evaluate. We have not established that every kinesin tail used in the screen can be induced to bind the split kinesin motor domain, although it seems likely that they all behave similarly. All of these kinesins have an N-terminal motor domain, which we removed and replaced with the FRB domain that is necessary to assemble the split kinesin. Because the expressed KIF5C motor domain is constitutively active, it builds up in the axon tips of the expressing cells and only a small fraction of the total motor is able to attach to vesicles in the soma. Therefore, low expression of the motor domain could lead to a negative result. Similarly, kinesin tail expression must be adequate to enable enough copies to bind to the vesicles, even in the presence of endogenous kinesins, to produce a clear change in transport once the split kinesin is assembled. However, this is not likely a problem in the experiments presented here, as we observed a strong positive interaction with one of the lower expressing kinesin tails, KIF13A.

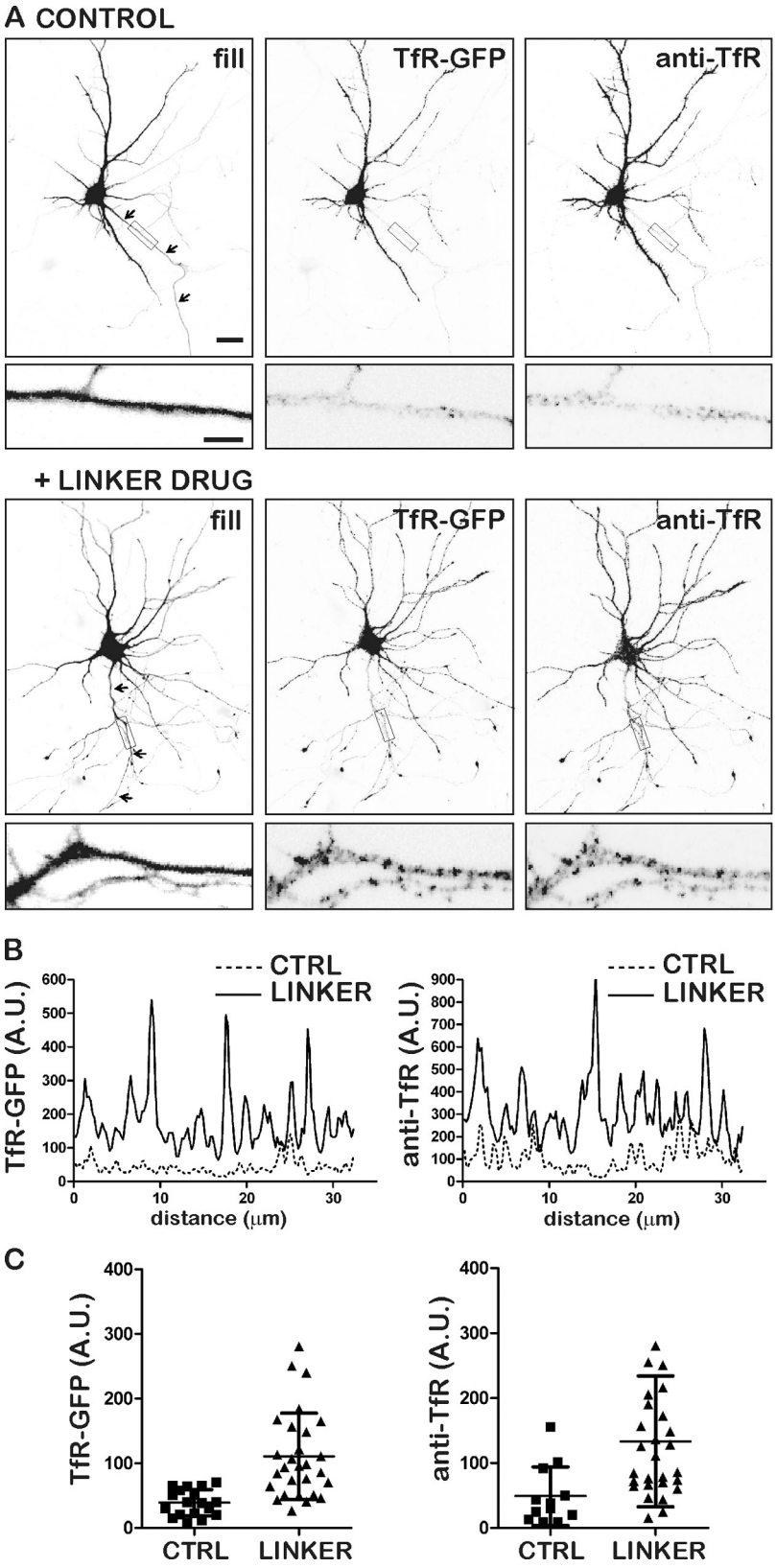

Figure 8. **Accumulation of misdirected TfR in the axon.** In cells expressing TfR-GFP, a KIF13B split kinesin, and soluble eBFP2 (to enable visualization of the entire axonal and dendritic arbor), incubation with the linker drug for 4 h significantly increased axonal TfR. To detect the TfR that reached the cell surface, live staining was performed using a monoclonal antibody against the extracellular GFP tag. (A) Representative control and treated cells showing the eBFP2 fill, TfR-GFP, and TfR that could be labeled from the cell surface in living cells. Note the prominent TfR fluorescence present in the treated cell. Bar, 20 µm. Boxed regions of the axon are shown at high magnification below. High magnification bar, 5 µm. (B) Line scans of the boxed regions of the axons in A show a pronounced increase in total TfR-GFP (left) and in TfR that reached the cell surface (right). A.U., arbitrary units. (C) Dot plots showing the average fluorescence intensity of TfR-GFP (left) and of TfR that could be labeled from the cell surface (right) in the axons of control cells and cells exposed to the linker drug (1 µM AP21967 for 4 h). Both total TfR and TfR that was accessible to extracellular antibody were significantly increased (*t* test, $P < 0.001$ and $P < 0.005$, respectively). Each point represents one cell; horizontal bars show means and SDs.

Further applications of the split kinesin approach

Adaptations of this method are likely to have a broad range of applications. We show that this method can be used in live-cell experiments as well as in fixed cells. Although the latter requires the induction of a considerable change in the distribution of the target vesicle, such fixed-cell experiments are far less time consuming than those that require live-cell imaging. In many cultured cells, microtubules are oriented with their minus ends near the centrosome and their plus ends near the cell

periphery. In such cells, assembly of a split kinesin would be expected to produce a redistribution of linked vesicles to the periphery that should be obvious in fixed cells. If desired, candidate kinesin tails could be linked to a minus end–directed kinesin motor domain or to a dynein, which would cause linked vesicles to aggregate near the cell center. Most kinesin–vesicle interactions are thought to be mediated by adaptors or scaffolding proteins, such as JIP1, GRIP-1, and mLin10 (Verhey et al., 2001; Setou et al., 2002; Guillaud et al., 2003). Rather than expressing FRB-tagged kinesin tails, one could use this assay to screen candidate kinesin adaptors modified to contain an FRB domain. The split kinesin method could also be used to investigate the regulation of kinesin–vesicle binding. For example, increased cytoplasmic calcium inhibits mitochondrial transport, but it is unclear whether calcium causes the kinesin to dissociate from the mitochondria or shifts the kinesin to an inactive state (Macaskill et al., 2009; Wang and Schwarz, 2009). The split kinesin approach could help in resolving this question.

In addition to investigating kinesin–vesicle interactions, it should be possible to adapt this assay to identify myosins and subunits of the dynein motor complex that bind a given vesicle population. The vesicle-binding domains of both myosins and dyneins could be tagged with FRB, allowing them to be linked to an appropriate FKBP-tagged kinesin motor domain that would result in a misdirection of the vesicles they bind. In yeast, expression of chimeras consisting of a myosin tail domain and a kinesin motor domain results in transport of myosin cargoes along microtubules (Lo Presti and Martin, 2011). Modifications of this assay could be used to identify any proteins thought to associate with vesicles, so long as creation of an FRB construct did not interfere with vesicle binding and enough copies were present and their association persisted long enough to move the vesicle. Finally, this experimental paradigm could also be used to determine whether two proteins colocalize on the same vesicle. By fusing an FRB to one of the proteins in question, that protein could be linked to an FKBP-tagged kinesin motor domain, leading to vesicle transport when the linker drug is added. The coordinated movement of both proteins would provide compelling evidence for colocalization.

The Kinesin-3 family and dendrite-selective vesicle transport

Our results show that KIF13A and KIF13B bind to dendritically polarized vesicles containing TfR and that KIF1A and KIF13B bind to dendritic vesicles containing LDLR. The association of KIF1A with dendritic vesicles was not unexpected. Previous work has shown that KIF1A associates with dendritically polarized AMPA receptors through the liprin-α cargo adaptor (Yonekawa et al., 1998; Shin et al., 2003). KIF1A is also a principal motor for transporting synaptic vesicle proteins in the axon and for transporting secretory granules in the axon and dendrites (Yonekawa et al., 1998; Lo et al., 2011). In accordance with these previous studies, we found that GFP-tagged KIF1A labels vesicles in both the axon and dendrites.

By comparison, the observation that KIF13A and KIF13B selectively bind dendritic vesicles was quite surprising. Neither of these kinesins has previously been implicated in dendritic transport. Little is known about cargoes carried by KIF13A, but it has been shown to interact with the AP-1 adaptor complex and to play a role in the transport of mannose-6-phopshate receptor (Nakagawa et al., 2000). KIF13B has previously been implicated in the transport of PIP_3 to growing axons at early stages of development, but it also interacts with an isoform of SAP97, which largely localizes to postsynaptic sites in dendrites (Rumbaugh et al., 2003; Horiguchi et al., 2006; Yoshimura et al., 2010). GFP-tagged KIF13B labels vesicles that are dendritically polarized—indeed, it is the only kinesin we have found that is exclusively associated with dendritic vesicles. Thus, the main role of KIF13B in mature neurons may be as a motor for dendritic transport.

Mechanisms underlying dendrite-selective transport

Selective transport is fundamental for the establishment and maintenance of neuronal polarity, but the underlying mechanisms and the role played by kinesin motors are still unclear. Two principal models have been proposed to explain the role of kinesins in selective dendritic transport. The "smart motor" hypothesis posits the existence of a subset of kinesins that can distinguish structural differences between axonal and dendritic microtubules and translocate preferentially to one or the other domain (Burack et al., 2000; Henthorn et al., 2011). Binding of a vesicle to a smart dendritic kinesin would of itself ensure its dendrite-selective transport. The alternative "cargo steering" or "cargo regulatory" hypothesis proposes that a single kinesin may mediate either axon- or dendrite-directed transport, depending on whether it interacts with a vesicle containing axonal or dendritic proteins (Setou et al., 2002). In support of this hypothesis, both KIF5 and KIF1A, which play a well-documented role in axonal transport, also interact with dendritically polarized glutamate receptors (Setou et al., 2002; Shin et al., 2003).

We show here that KIF1A interacts with dendritically polarized LDLR vesicles. These results are inconsistent with the smart motor hypothesis. KIF13A, which is present on dendrite-selective TfR-containing vesicles, also associates with vesicles that are transported into the axon (Fig. 2), although the cargo contained in these vesicles has not yet been identified. A recent study in *Drosophila* showed that Khc, a member of the Kinesin-1 family, participates in the dendrite-selective transport of some cargoes and mediates axonal transport of other cargoes (Henthorn et al., 2011). Of all the kinesins we examined, only KIF13B has some of the characteristics of a smart motor—GFP-tagged KIF13B is associated with vesicles that are largely confined to the somatodendritic domain. However, the motor domain of KIF13B is capable of walking on axonal microtubules, which suggests that other factors also regulate the translocation selectivity of this kinesin (Huang and Banker, 2011).

The axon initial segment marks the boundary between the axonal and somatodendritic domains and vesicles carrying dendritic proteins do not proceed beyond this boundary (Burack et al., 2000; Rasband, 2010). Several models suggest that the transport of dendritic vesicles is inhibited when they reach this region of the cell, either due to entrapment in an actin meshwork (Song et al., 2009), to the action of myosins that link dendritic vesicles to actin filaments (Lewis et al., 2009), or to a change in

the balance between kinesin- and dynein-based motility. Finally, entry into the axon may depend on whether or not a kinesin walks efficiently on the unique subset of microtubules that traverse the initial segment (Nakata and Hirokawa, 2003; Leterrier et al., 2011; Nakata et al., 2011). The results presented here impact all of these models. Any model of selective transport must explain how kinesins are prevented from entering the axon when they carry a dendritic vesicle but are perfectly capable of passing through the initial segment when they carry an axonal vesicle. Elucidating the molecular mechanisms that enable cargo binding to regulate kinesin translocation will be essential in refining our understanding of selective vesicle transport.

Materials and methods

Cell culture

Primary hippocampal neurons were prepared as described previously (Kaech and Banker, 2006; Kaech et al., 2012). Hippocampi were dissected from E18 rats, trypsinized, dissociated, and plated on poly-L-lysine-treated 18-mm glass coverslips. Cultures were grown in minimal essential medium with N2 supplements and maintained at 37°C in an incubator with a 5% CO_2 atmosphere. Constructs were transfected into stage 4 hippocampal neurons (8–12 d in culture) using Lipofectamine 2000 (Invitrogen) and allowed to express for 8–18 h before imaging.

Constructs

Full-length plus end–directed kinesins consist of an N-terminal motor domain that interacts with microtubules, which is directly followed by a neck linker and a coiled-coil that facilitates dimerization. The motor domain used in all experiments was KIF5C^{559}-tdTM-FKBP. KIF5C^{559} homodimerizes and forms a constitutively active motor that moves to the plus end of microtubules (Friedman and Vale, 1999; Jacobson et al., 2006). Kinesin tails were all engineered following the same strategy: The N-terminal motor domain was removed and replaced with an FRB-3myc domain (see Table 1 for details). All constructs were cloned into the pCAG expression vector.

The linkage of tail to the active motor domain was induced by treating cells expressing motor and tail constructs with AP 21967, a rapamycin analogue (Muthuswamy et al., 1999; Kapitein et al., 2010). Human TfR (NCBI protein database accession no. M11507) was tagged with eGFP at its C terminus (Jareb and Banker, 1998; Burack et al., 2000; Silverman et al., 2001); human LDLR (GenBank/EMBL/DDBJ accession no. NM_000527) was N-terminally tagged by insertion of eGFP downstream of the signal sequence.

Imaging

During live imaging, cells were maintained at 32–34°C in a heated chamber (Warner Instruments) containing Hibernate E without phenol red (BrainBits) supplemented with B27 (Invitrogen). Objectives were warmed to 34°C (Bioptechs Inc.). Images were acquired using a microscope (model TE2000; Nikon) equipped with a spinning-disk confocal-head (model CSU10, Yokogawa Corporation of America; Solamere Technology Group, Salt Lake City, UT) and were captured with a CCD camera (Orca-ER; Hamamatsu Photonics). Samples were illuminated with a KrAr ion laser (Innova 70C; Coherent, Inc.). A Plan-Apo 60x 1.45 NA objective (Nikon) was used to acquire image streams. During image acquisition, z axis movement was controlled by the Perfect Focus system on the TE2000 microscope (Nikon). Image streams of 60–90 frames (600–750 ms/frame) were acquired before drug addition and at 10–15-min intervals after adding the dimerizing drug. For further details, see Kaech et al. (2012). Images for Fig. 2 were obtained using a microscope (model DM RXA; Leica) with a 63x Plan-Apo 1.32 NA objective and were captured using a CCD camera (Micromax; Princeton Instruments). Cells were maintained as above but using imaging media consisting of HBSS with Ca^{2+}, Mg^{2+}, and 10 mM Hepes (Gibco) with 0.6% glucose. MetaMorph software (Molecular Devices) was used to drive microscopes and analyze movies.

Images of fixed cells were acquired with a microscope (Observer Z1; Carl Zeiss) and AxioVision software (Carl Zeiss) using an LCI Plan-Apochromat 63x/1.4 NA objective and an Axiocam MRm camera (Carl Zeiss). Mosaic images were acquired using MosaiX function of AxioVision and aligned using MetaMorph. In all figures, the contrast has been reversed so that fluorescent objects appear dark on a light background.

Antibody staining

To detect expressed TfR-GFP that could be labeled from the cell surface, living neurons were incubated in primary antibody against GFP (Roche) diluted 1:100 in culture medium for 7–10 min at 37°C. Coverslips were then rinsed in PBS, fixed in 4% paraformaldehyde/4% sucrose in PBS and permeabilized with 0.25% Triton X-100 in PBS. Cells were incubated in 0.50% fish skin gelatin (Sigma-Aldrich) in PBS for 1 h at 37°C to block nonspecific antibody-binding sites. Coverslips were then incubated in Alexa Fluor 555–conjugated secondary antibody (Invitrogen) for 1 h at 37°C.

To evaluate the expression levels of split kinesin tails, neurons expressing each of the tail constructs were fixed and permeabilized as described above. The Myc epitope tag was detected by incubating cultures for 1 h at room temperature with primary antibody 9E10 (Sigma-Aldrich) diluted 1:350. The cells were washed, then incubated for 45 min with Alexa Fluor 488–conjugated secondary antibody (Invitrogen).

Quantification

For quantification of vesicle transport, time-distance "kymographs" of vesicle motion were generated using MetaMorph software. To determine the number of anterograde events, positively sloped lines were traced on the kymographs and the coordinates of these regions were transferred to an Excel spreadsheet. Anterograde events that extended at least 3 µm were counted. This analysis was completed by an observer who was blinded to the identity of the kinesin tail expressed and whether or not cells had been exposed to the linker drug.

To quantify the fluorescence of TfR-GFP and anti-GFP staining to detect cell surface TfR-GFP, two regions (proximal and medial) were drawn on the axons using the soluble eBFP2 signal as a guide. A threshold was applied to these regions, then they were transferred to the TfR images and the average fluorescence for each region was calculated. An average background fluorescence value was determined from several regions containing unlabeled neurites and subtracted from the average intensity of the axon. At least 10 cells were evaluated per condition from at least two different cultures.

To quantify expression of myc-tagged kinesin tails, a region was drawn around the cell body using the soluble eBFP2 signal as a guide. A threshold was applied to this region, then it was transferred to the myc image and the average fluorescence was calculated. An average background fluorescence value was determined from several regions containing unlabeled cell bodies. A minimum of 15 cells was evaluated per condition from at least two different cultures.

Online supplemental material

Video S1 shows that axonal transport of FRB-GFP-KIF1A–labeled vesicles increases rapidly after they are linked to a constitutively active, axonally targeted kinesin motor domain. Video S2 shows that axonal transport of TfR-GFP–labeled vesicles increases rapidly after they are linked to a constitutively active axonal motor through the FRB-3myc-KIF13B tail. Online supplemental material is available at http://www.jcb.org/cgi/content/full/jcb.201205070/DC1.

We thank Barbara Smoody for her outstanding technical assistance and Dr. Stefanie Kaech for her advice on imaging. We also thank Drs. Cheng Fang, Ann Marie Craig, Bruce Schnapp, Richard Goodman, and Peter Gillespie for their comments on the manuscript.

This work was supported by National Institutes of Health (NIH) grant MH066179; live-cell imaging was conducted at the Advanced Light Microscopy Core at The Jungers Center, which is supported in part by NIH grant P30-NS06180 (S. Aicher, principle investigator). H. Decker was the recipient of the McDonald fellowship from the Multiple Sclerosis International Federation.

Submitted: 11 May 2012
Accepted: 13 July 2012

References

Akhmanova, A., and J.A. Hammer III. 2010. Linking molecular motors to membrane cargo. *Curr. Opin. Cell Biol.* 22:479–487. http://dx.doi.org/10.1016/j.ceb.2010.04.008

Belshaw, P.J., S.N. Ho, G.R. Crabtree, and S.L. Schreiber. 1996. Controlling protein association and subcellular localization with a synthetic ligand that induces heterodimerization of proteins. *Proc. Natl. Acad. Sci. USA*. 93:4604–4607. http://dx.doi.org/10.1073/pnas.93.10.4604

Burack, M.A., M.A. Silverman, and G. Banker. 2000. The role of selective transport in neuronal protein sorting. *Neuron*. 26:465–472. http://dx.doi.org/10.1016/S0896-6273(00)81178-2

Chu, P.J., J.F. Rivera, and D.B. Arnold. 2006. A role for Kif17 in transport of Kv4.2. *J. Biol. Chem.* 281:365–373. http://dx.doi.org/10.1074/jbc.M508897200

Friedman, D.S., and R.D. Vale. 1999. Single-molecule analysis of kinesin motility reveals regulation by the cargo-binding tail domain. *Nat. Cell Biol.* 1:293–297. http://dx.doi.org/10.1038/13008

Gan, Y., T.E. McGraw, and E. Rodriguez-Boulan. 2002. The epithelial-specific adaptor AP1B mediates post-endocytic recycling to the basolateral membrane. *Nat. Cell Biol.* 4:605–609.

Guillaud, L., M. Setou, and N. Hirokawa. 2003. KIF17 dynamics and regulation of NR2B trafficking in hippocampal neurons. *J. Neurosci.* 23:131–140.

Henthorn, K.S., M.S. Roux, C. Herrera, and L.S. Goldstein. 2011. A role for kinesin heavy chain in controlling vesicle transport into dendrites in *Drosophila*. *Mol. Biol. Cell*. 22:4038–4046. http://dx.doi.org/10.1091/mbc.E10-07-0572

Hirokawa, N., and Y. Noda. 2008. Intracellular transport and kinesin superfamily proteins, KIFs: structure, function, and dynamics. *Physiol. Rev.* 88:1089–1118. http://dx.doi.org/10.1152/physrev.00023.2007

Hirokawa, N., S. Niwa, and Y. Tanaka. 2010. Molecular motors in neurons: transport mechanisms and roles in brain function, development, and disease. *Neuron*. 68:610–638. http://dx.doi.org/10.1016/j.neuron.2010.09.039

Horiguchi, K., T. Hanada, Y. Fukui, and A.H. Chishti. 2006. Transport of PIP3 by GAKIN, a kinesin-3 family protein, regulates neuronal cell polarity. *J. Cell Biol.* 174:425–436. http://dx.doi.org/10.1083/jcb.200604031

Huang, C.F., and G. Banker. 2011. The translocation selectivity of the kinesins that mediate neuronal organelle transport. *Traffic*. 13:549–564. http://dx.doi.org/10.1111/j.1600-0854.2011.01325.x

Jacobson, C., B. Schnapp, and G.A. Banker. 2006. A change in the selective translocation of the Kinesin-1 motor domain marks the initial specification of the axon. *Neuron*. 49:797–804. http://dx.doi.org/10.1016/j.neuron.2006.02.005

Jareb, M., and G. Banker. 1998. The polarized sorting of membrane proteins expressed in cultured hippocampal neurons using viral vectors. *Neuron*. 20:855–867. http://dx.doi.org/10.1016/S0896-6273(00)80468-7

Kaech, S., and G. Banker. 2006. Culturing hippocampal neurons. *Nat. Protoc.* 1:2406–2415. http://dx.doi.org/10.1038/nprot.2006.356

Kaech, S., C.F. Huang, and G. Banker. 2012. Short-term high-resolution imaging of developing hippocampal neurons in culture. *Cold Spring Harb Protoc*. 2012:340–343.

Kapitein, L.C., M.A. Schlager, M. Kuijpers, P.S. Wulf, M. van Spronsen, F.C. MacKintosh, and C.C. Hoogenraad. 2010. Mixed microtubules steer dynein-driven cargo transport into dendrites. *Curr. Biol.* 20:290–299. http://dx.doi.org/10.1016/j.cub.2009.12.052

Kennedy, M.J., I.G. Davison, C.G. Robinson, and M.D. Ehlers. 2010. Syntaxin-4 defines a domain for activity-dependent exocytosis in dendritic spines. *Cell*. 141:524–535. http://dx.doi.org/10.1016/j.cell.2010.02.042

Lee, J.R., H. Shin, J. Ko, J. Choi, H. Lee, and E. Kim. 2003. Characterization of the movement of the kinesin motor KIF1A in living cultured neurons. *J. Biol. Chem.* 278:2624–2629. http://dx.doi.org/10.1074/jbc.M211152200

Leterrier, C., H. Vacher, M.P. Fache, S.A. d'Ortoli, F. Castets, A. Autillo-Touati, and B. Dargent. 2011. End-binding proteins EB3 and EB1 link microtubules to ankyrin G in the axon initial segment. *Proc. Natl. Acad. Sci. USA*. 108:8826–8831. http://dx.doi.org/10.1073/pnas.1018671108

Lewis, T.L. Jr., T. Mao, K. Svoboda, and D.B. Arnold. 2009. Myosin-dependent targeting of transmembrane proteins to neuronal dendrites. *Nat. Neurosci.* 12:568–576. http://dx.doi.org/10.1038/nn.2318

Lo, K.Y., A. Kuzmin, S.M. Unger, J.D. Petersen, and M.A. Silverman. 2011. KIF1A is the primary anterograde motor protein required for the axonal transport of dense-core vesicles in cultured hippocampal neurons. *Neurosci. Lett.* 491:168–173. http://dx.doi.org/10.1016/j.neulet.2011.01.018

Lo Presti, L., and S.G. Martin. 2011. Shaping fission yeast cells by rerouting actin-based transport on microtubules. *Curr. Biol.* 21:2064–2069. http://dx.doi.org/10.1016/j.cub.2011.10.033

Macaskill, A.F., J.E. Rinholm, A.E. Twelvetrees, I.L. Arancibia-Carcamo, J. Muir, A. Fransson, P. Aspenstrom, D. Attwell, and J.T. Kittler. 2009. Miro1 is a calcium sensor for glutamate receptor-dependent localization of mitochondria at synapses. *Neuron*. 61:541–555. http://dx.doi.org/10.1016/j.neuron.2009.01.030

Maxfield, F.R., and T.E. McGraw. 2004. Endocytic recycling. *Nat. Rev. Mol. Cell Biol.* 5:121–132. http://dx.doi.org/10.1038/nrm1315

May, P., E. Woldt, R.L. Matz, and P. Boucher. 2007. The LDL receptor-related protein (LRP) family: an old family of proteins with new physiological functions. *Ann. Med.* 39:219–228. http://dx.doi.org/10.1080/07853890701214881

Muthuswamy, S.K., M. Gilman, and J.S. Brugge. 1999. Controlled dimerization of ErbB receptors provides evidence for differential signaling by homo- and heterodimers. *Mol. Cell. Biol.* 19:6845–6857.

Nakagawa, T., M. Setou, D. Seog, K. Ogasawara, N. Dohmae, K. Takio, and N. Hirokawa. 2000. A novel motor, KIF13A, transports mannose-6-phosphate receptor to plasma membrane through direct interaction with AP-1 complex. *Cell*. 103:569–581. http://dx.doi.org/10.1016/S0092-8674(00)00161-6

Nakata, T., and N. Hirokawa. 2003. Microtubules provide directional cues for polarized axonal transport through interaction with kinesin motor head. *J. Cell Biol.* 162:1045–1055. http://dx.doi.org/10.1083/jcb.200302175

Nakata, T., S. Niwa, Y. Okada, F. Perez, and N. Hirokawa. 2011. Preferential binding of a kinesin-1 motor to GTP-tubulin-rich microtubules underlies polarized vesicle transport. *J. Cell Biol.* 194:245–255. http://dx.doi.org/10.1083/jcb.201104034

Rasband, M.N. 2010. The axon initial segment and the maintenance of neuronal polarity. *Nat. Rev. Neurosci.* 11:552–562. http://dx.doi.org/10.1038/nrn2852

Rumbaugh, G., G.M. Sia, C.C. Garner, and R.L. Huganir. 2003. Synapse-associated protein-97 isoform-specific regulation of surface AMPA receptors and synaptic function in cultured neurons. *J. Neurosci.* 23:4567–4576.

Setou, M., T. Nakagawa, D.H. Seog, and N. Hirokawa. 2000. Kinesin superfamily motor protein KIF17 and mLin-10 in NMDA receptor-containing vesicle transport. *Science*. 288:1796–1802. http://dx.doi.org/10.1126/science.288.5472.1796

Setou, M., D.H. Seog, Y. Tanaka, Y. Kanai, Y. Takei, M. Kawagishi, and N. Hirokawa. 2002. Glutamate-receptor-interacting protein GRIP1 directly steers kinesin to dendrites. *Nature*. 417:83–87. http://dx.doi.org/10.1038/nature743

Shin, H., M. Wyszynski, K.H. Huh, J.G. Valtschanoff, J.R. Lee, J. Ko, M. Streuli, R.J. Weinberg, M. Sheng, and E. Kim. 2003. Association of the kinesin motor KIF1A with the multimodular protein liprin-alpha. *J. Biol. Chem.* 278:11393–11401. http://dx.doi.org/10.1074/jbc.M211874200

Silverman, M.A., S. Kaech, M. Jareb, M.A. Burack, L. Vogt, P. Sonderegger, and G. Banker. 2001. Sorting and directed transport of membrane proteins during development of hippocampal neurons in culture. *Proc. Natl. Acad. Sci. USA*. 98:7051–7057. http://dx.doi.org/10.1073/pnas.111146198

Silverman, M.A., S. Kaech, E.M. Ramser, X. Lu, M.R. Lasarev, S. Nagalla, and G. Banker. 2010. Expression of kinesin superfamily genes in cultured hippocampal neurons. *Cytoskeleton (Hoboken)*. 67:784–795.

Song, A.H., D. Wang, G. Chen, Y. Li, J. Luo, S. Duan, and M.M. Poo. 2009. A selective filter for cytoplasmic transport at the axon initial segment. *Cell*. 136:1148–1160. http://dx.doi.org/10.1016/j.cell.2009.01.016

Terada, S., and N. Hirokawa. 2000. Moving on to the cargo problem of microtubule-dependent motors in neurons. *Curr. Opin. Neurobiol.* 10:566–573. http://dx.doi.org/10.1016/S0959-4388(00)00129-X

Verhey, K.J., D. Meyer, R. Deehan, J. Blenis, B.J. Schnapp, T.A. Rapoport, and B. Margolis. 2001. Cargo of kinesin identified as JIP scaffolding proteins and associated signaling molecules. *J. Cell Biol.* 152:959–970. http://dx.doi.org/10.1083/jcb.152.5.959

Verhey, K.J., N. Kaul, and V. Soppina. 2011. Kinesin assembly and movement in cells. *Annu Rev Biophys*. 40:267–288. http://dx.doi.org/10.1146/annurev-biophys-042910-155310

Wang, X., and T.L. Schwarz. 2009. The mechanism of Ca2+ -dependent regulation of kinesin-mediated mitochondrial motility. *Cell*. 136:163–174. http://dx.doi.org/10.1016/j.cell.2008.11.046

Yonekawa, Y., A. Harada, Y. Okada, T. Funakoshi, Y. Kanai, Y. Takei, S. Terada, T. Noda, and N. Hirokawa. 1998. Defect in synaptic vesicle precursor transport and neuronal cell death in KIF1A motor protein-deficient mice. *J. Cell Biol.* 141:431–441. http://dx.doi.org/10.1083/jcb.141.2.431

Yoshimura, Y., T. Terabayashi, and H. Miki. 2010. Par1b/MARK2 phosphorylates kinesin-like motor protein GAKIN/KIF13B to regulate axon formation. *Mol. Cell. Biol.* 30:2206–2219. http://dx.doi.org/10.1128/MCB.01181-09